

Learning intrinsic excitability in medium spiny neurons

Gabriele Scheler¹ and Johann Schumann²

¹ISLE Stanford, Ca 94305 and ²RIACS NASA Ames, Ca 94035

Abstract

We present an unsupervised, local activation-dependent learning rule for intrinsic plasticity (IP) which affects the composition of ion channel conductances for single neurons in a use-dependent way.

We use a single-compartment conductance-based model for medium spiny striatal neurons in order to show the effects of parametrization of individual ion channels on the neuronal activation function. We show that parameter changes within the physiological ranges are sufficient to create an ensemble of neurons with significantly different activation functions. We emphasize that the effects of intrinsic neuronal variability on spiking behavior require a distributed mode of synaptic input and can be eliminated by strongly correlated input.

We show how variability and adaptivity in ion channel conductances can be utilized to store patterns without an additional contribution by synaptic plasticity (SP). The adaptation of the spike response may result in either "positive" or "negative" pattern learning. However, read-out of stored information depends on a distributed pattern of synaptic activity to let intrinsic variability determine spike response. We briefly discuss the implications of this conditional memory on learning and addiction.

Keywords: single neuron model, striatal medium spiny neuron, ion channels, activation function, unsupervised learning, intrinsic plasticity, pattern learning, neuronal variability

Introduction

A role for modification of activation functions, or intrinsic plasticity (IP), for behavioral learning

has been demonstrated for a number of systems [Zhang and Linden, 2003]. For instance, in rabbit eye-blink conditioning, when ion channels related to afterhyperpolarization are being suppressed by a learning event, they can become permanently suppressed. This has been shown for pyramidal cells of hippocampal areas CA1 and CA3, and for cerebellar Purkinje cells [Schreurs et al., 1998]. In some cases, these changes are permanent and still present after 30 days [Moyer et al., 1996, Thompson et al., 1996], in other cases, intrinsic changes disappear after 3-7 days, while the behavioral memory remains intact, raising questions about the long-term component of intrinsic plasticity in these systems. There are at the present time conflicting ideas on the significance of IP compared to synaptic plasticity [Zhang and Linden, 2003], and the range of functions that IP may have in adaptivity [Destexhe and Marder, 2004].

Few computational models have been proposed that show how modification in activation functions can be achieved with ion channel based models of realistic single neurons. Marder and colleagues have developed an approach, where they sample a very large parameter space for conductances of ion channels, exploring nonlinearities in the relation between conductances and neural spiking behavior [Goldman et al., 2001, Prinz and Marder, 2004]. The motivation for this research are observations about neuromodulation and intrinsic plasticity in specific neurons of an invertebrate ganglion (e.g., [LeMasson et al., 1993]). They have noted that large variations in some parameters may have little effect on neuronal behavior, while comparatively small variations in certain regions in parameter space may change response properties significantly. They also suggest that neuromodulation may provide an efficient means of targeting regions in parameter

space with significant effects on response properties [Goldman et al., 2001].

A study by [Stemmler and Koch, 1999] assumed the goal of modification of activation functions is to achieve an optimal distribution of firing rates for a population of neurons. The idea was that by tuning each neuron to a different band of the frequency spectrum, the full bandwidth of frequencies could be employed for information transfer. This goal was achieved by adjusting Na^+ , K^+ and Ca^{++} channels for a generically defined neuron until a desired frequency was stably reached.

We present a different approach, where the modification of activation functions reflects the history of exposure to stimuli for a specific neuron. Similarly, [Daoudal and Debanne, 2003] suggested that synaptic LTP/LTD and linear regulations of intrinsic excitability could operate in a synergistic fashion. However, in our approach, different types of synaptic stimulation result in state changes for the neuronal unit, influencing its capacity for read-out of stored intrinsic properties. Thus, intrinsic plasticity is conceptualized as fundamentally different from LTP/LTD which does not encompass such a state change. The learning rule that we derive as the basis for adjustment concerns one-dimensional upregulation or downregulation of excitability in the "read-out" state of the neuron, and affecting only this state. This rule uses neural activation, significantly determined by intracellular calcium for the learning parameter, which can be shown to be biologically well-motivated (cf. also [LeMasson et al., 1993]).

Materials and Methods

Striatal medium spiny neuron

The membrane voltage V_m is modeled as $\dot{V}_m = -\frac{1}{C}[\sum_i I_i - I_{syn}]$. The individual currents are modeled by conductances, state variables and the reversal potential:

$$I_i = \bar{g}_i(V_m) * m^{p_i} * h_i^{q_i} * (V_m - E_i^{rev}) \quad (1)$$

The dynamics are defined using state variables for activation (m) and inactivation (h). The types of equa-

tions used for the dynamics are:

1. exponential: $f(V_m) = \lambda \exp(\frac{V_m - V_i}{-V_c})$
2. logistic: $f(V_m) = \frac{\lambda}{1 + \exp(\frac{V_m - V_i}{-V_c})}$
3. linexp: $f(V_m) = \frac{\lambda(V_m - V_i)}{1 + \exp(\frac{V_m - V_i}{-V_c})}$

The state variables can be defined indirectly using

$$\dot{m} = (1 - m)\alpha - m\beta$$

and

$$\dot{h} = (1 - h)\alpha - h\beta$$

and one of the equations (1-3) with different values for λ ($\lambda_\alpha, \lambda_\beta$), V_i (V_i^α, V_i^β) and V_c (V_c^α, V_c^β). We use this method for the ion channels in Table 1.

The state variables can also be directly defined (cf. [Goldman et al., 2001]):

$$\dot{m} = \frac{m_\infty - m}{\tau_m}$$

$$\dot{h} = \frac{h_\infty - h}{\tau_h}$$

The parameters used are $m_\infty = m_0$, $h_\infty = h_0$, τ_m and τ_h as in Table 2. Again, we use one of the equations (1-3) with the λ parameters (λ_{m0} and λ_{h0}) set to 1.

(These representations are mathematically equivalent and related by $m_\infty = \frac{\alpha_m}{\alpha_m + \beta_m}$, $\tau_\infty = \frac{1}{\alpha_m + \beta_m}$.)

Standard parameter values for the modeling of ion channels ('naive state') were compared with several publications. Parameter values for I_K , I_{Na} and I_{leak} were adapted from [Wang and Buzsaki, 1996], for L-type calcium channels (I_{CaL}) from [Bargas et al., 1994] and [Tsubo et al., 2004], see Table 1.

Parameters for slow A-type K channels (I_{As}) were adapted from [Gabel and Nisenbaum, 1998, Nisenbaum et al., 1998], for fast A-type K channels (I_{Af}) from [Surmeier et al., 1989], for inward rectifying K channels (I_{Kir}) from [Nisenbaum and Wilson, 1995], and the resulting parameter tables were compared with [Mahon et al., 2000b] and [Gruber et al., 2003], see Table 2.

Variability

The maximum conductance of different ion channels can be expressed by a scaling factor in the membrane potential equations as in Eq. 2 (for synaptic currents) or Eq. 3 (for synaptic conductances), cf. [Gruber et al., 2003].

$$\dot{V}_m = -\frac{1}{C}[\mu_1 I_1 + \mu_2 I_2 \dots + \mu_i I_i - I_{syn}] \quad (2)$$

$$\dot{V}_m = -\frac{1}{C}[\mu_1 I_1 + \dots + g_s(V_m - V_0)] \quad (3)$$

Both NM-independent and NM-dependent modifications may coexist in a neuron, as expressed in Eq. 4 ([NM] stands for the level of synaptic availability of a neuromodulator NM).

$$\dot{V}_m = -\frac{1}{C}[(\mu_1 I_1 + [NM]\kappa_1 I_1) + (\mu_2 I_2 + [NM]\kappa_2 I_2) \dots] \quad (4)$$

In this paper, for simplicity, we shall refer to (Eq. 2) as the generic format for intrinsic adaptation, with the understanding that μ is replaceable by $[NM]\kappa$.

Physiological ranges for μ can be estimated by various means. There are measurements for variability in electrophysiologically defined membrane behavior (current threshold, spike response to current pulses etc. [Onn et al., 2003, Mahon et al., 2000a]) that are typically expressed as standard errors (e.g. 16-20% for current threshold, [Onn et al., 2003]). There are also attempts at classifying MSN cells into different 'types' based on their electrophysiological profile [Wickens and Wilson, 1998, Onn et al., 2000]. Modeling shows that variability of ion channel conductances with a range of $\pm 40\%$ matches measures of electrophysiological variability and reproduces the ranges for MSN types (data not shown). Interestingly, direct measurements for dopamine D1 receptor-mediated changes on ion channel conductances are approximately in the same ranges ($\pm 30 - 40\%$, [Gruber et al., 2003]). Our discussion is thus based on an estimate of μ ranging from 0.6 - 1.4 for each channel.

Defining synaptic input

Synaptic input is defined by overlays of the EPSPs generated by N individual Poisson-distributed spike trains with mean interspike interval τ_{syn} . Each EPSP is modeled as a spike with peak amplitude $I_0 = 1.2\mu A/cm^2$ and exponential decay with $\tau = 2.5ms$ similar to [Tsubo et al., 2004, Sachdev et al., 2004]. IPSPs are modeled in a similar way with $I_0 = -0.4\mu A/cm^2$. This corresponds to 0.5nA (-0.2nA) as peak current (with $1nA = 2.3\mu A/cm^2$). Synaptic conductances are calculated by $g_{syn} = I_{syn}/(V_m - V_0)$ with V_0 set to 0mV. We have tuned the model to $g_{syn} = 0.0035mS/cm^2$ for a first spike for the naive or standard neuron (all $\mu = 1$). At -40mV, this is $0.0035mS/cm^2 * (-40mV) = -1.4\mu A/cm^2$ or $0.6nA$, which corresponds to the experimentally measured average value for the rheobase in [Onn et al., 2003]. We may increase the correlation in the input by using a percentage W of neurons which fire at the same time. Higher values for W increase the amplitude of the fluctuations of the input (cf. [Benucci et al., 2004]).

Implementation

The simulator has been implemented in Matlab and executed on an Apple 1GHz G4 notebook. The entire code is interpreted and no specific code optimizations have been applied. For numerical integration, the solver ode45 was used. Simulation of one neuron for 1 s took approximately 68s CPU time. It is expected that for compiled and optimized code the simulation speed could be increased by at least an order of magnitude.

Results

Intrinsic Variability

We explore the impact of small variations in ion channel conductances on the shape of the activation function. As an example, we show the current and conductance changes for a slowly inactivating A-type K+ channel ($Kv1.2$, I_{As}), L-type calcium channel (I_{CaL}) and inward rectifying K+ channel (I_{Kir}) at different membrane potentials modulated by a scaling factor

$\mu = \{0.6, 0.8, 1.0, 1.2, 1.4\}$ (Fig. 1, Fig. 2). Regulation of the voltage-dependence [Misonou et al., 2004] and even of the inactivation dynamics of an ion channel [Hayashida and Ishida, 2004] has also been shown, but these effects are not further discussed here.

We can see that there are critical voltage ranges (around -50mV, around -80mV and starting at -40mV), where the conductance and the current are highest, and where scaling has a significant effect, while scaling has small or no effect in other voltage ranges. (The Na+ current has been disabled for this example to prevent the neuron from firing).

In Fig. 3, we show the current over time - to graphically display the slow dynamics of the I_{As} and I_{CaL} channel. Since we do not change the activation-inactivation dynamics of any channel in our model, we show currents only for $\mu_{As}, \mu_{CaL} = 1$.

We can see that I_{As} activates moderately fast (20ms), while it inactivates with a half-time of about 300ms, depending on the voltage. For I_{CaL} , activation is almost instantaneous, but inactivation is > 500 ms.

The activation function for the MSN model shows a time-dependence only in the high-voltage range (at or above -55mV), whereas the components in the lower voltage ranges are not time-dependent.

Mathematically, we can consider the individual channels as a set of basis functions that allow function approximation for the activation function. Each particular adjustment of an activation function can be considered learning of a filter which is suited to a specific processing task. The activation-inactivation dynamics would provide a similar set of basis functions for the temporal domain. Of course, it is interesting to note which particular basis functions exist, and also how the temporal dimension is tied in with specific voltage-dependences. For instance, the slowly inactivating potassium channel I_{As} provides a skewed mirror image of the function of calcium-gated Sk/BK channels, which are responsible for afterhyperpolarization, making different variants of frequency filters possible. On this basis, a mapping of ion channel components and their density or distributions in different types of neurons could provide an interesting perspective on direct interactions for neurons from different tissue types or brain areas, as well as e.g. between cholinergic interneurons and MSNs within striatum.

To further explore the influence of variability of the activation function, we apply realistic synaptic input with different amounts of correlation to individual MS neurons (see Fig. 4).

This shows us that small adjustments in the contribution of a specific ion channel can result in significantly different spiking behavior even for identical synaptic input. This occurs when the input is distributed, i.e. has low correlation. In this case, the neurons spike independently of each other and with different frequencies. We can eliminate this effect by increasing the correlation of the input. Because of the slow activation/inactivation dynamics of the I_{As} channel, (latency of ≈ 20 ms) only low correlated input activates these channels ('neuronal integrator mode'), but highly correlated inputs do not activate these channels, driving the membrane to spiking quickly ('coincidence detector mode'). Therefore correlated input can produce reliable spiking behavior for model neurons which differ in the relative contribution of the slow I_{As} channel. Distributed input, in contrast, activates slower ion channels, and can produce different tonic firing rates, here according to the contribution of the I_{As} channels, as long as strong synaptic input keeps the neuron in the relevant voltage range ('persistent activity').

Similarly, the differential contribution of other channels (high-voltage gated L-type Ca-channels, hyperpolarization-activated GIRK channels or calcium-dependent Sk/Bk channels) will affect neuronal behavior, when the conditions for a prominent influence of these channels are met.

We are modeling a state of MS neurons that exhibits regular tonic firing. In experimental studies, [Wilson and Kawaguchi, 1996] showed that MS neurons, similar to cortical neurons, exhibit upstate-downstate behavior, reminiscent of slow-wave sleep, under certain forms of anesthesia (ketamine, barbiturate). However, under neurolept-analgesia (fentanyl-haloperidol), [Mahon et al., 2003] showed that MS neurons can show driven activity, when cortical input is highly synchronized, and exhibit a state characterized by fluctuating synaptic inputs without rhythmic activity (i.e. without upstates/downstates), when cortical input is desynchronized. The regular, tonic spiking in this state is very low, much less than in the waking animal, which may be related to the dopamine

block by haloperidol. This makes a waking state of MS neurons characterized by regular tonic spiking at different firing rates probable.

In the following, we show how intrinsic excitability adaptation can lead to different recalled firing rates under appropriate synaptic stimulation. The model could thus reflect learning that is recalled or read out during MSN states under desynchronized cortical input - in contrast to highly synchronized input, which would homogenize the response of the coincidence detecting neurons and favor reliable transfer of spikes.

Induction and Maintenance of Plasticity

The general idea for learning intrinsic plasticity is to use a learning parameter h for each individual update of the conductance scaling factor μ . The *direction* of learning ($h > 0$ or $h < 0$) is determined from the neural activation (A_n) for each individual neuron. Neural activation is largely determined by intracellular calcium but here we estimate the neural activation A_n from the spike rate of the neuron, measured over 1 s of simulated behavior (see for a discussion).

We define a bidirectional learning rule dependent on an initial firing rate θ : excitability is increased by a step function h (with stepsize σ) when A_n is greater than θ , excitability is decreased when A_n is lower than θ ("positive learning"). This means, when the actual neural activation is higher than the initial firing rate, membrane adaptations aim to move the neuron to a higher excitability in order to create a positive memory trace of a period of high activation (which can then be replicated under distributed synaptic stimulation). The same mechanism applies to lower the excitability of a neuron.

$$\begin{aligned} \Delta\mu &= h(A_n) = \sigma & \text{if } A_n > \theta \\ \Delta\mu &= h(A_n) = -\sigma & \text{if } A_n < \theta \end{aligned} \quad (5)$$

This rule can also be implemented by individual increases in excitability after each action potential, and decreases of excitability for periods of time without action potentials. Initial experiments [Mahon et al., 2003, Zhang et al., 2004] indeed show such adaptation of intrinsic excitability after individual spikes.

The function h can be applied to a single ion channel, such as I_{As} , but also to a number of ion channels in parallel: e.g. to mimic dopamine D1 receptor activation, h may be applied to μ_{As} (upregulated with high A_n), μ_{Na} (downregulated with high A_n), and μ_{CaL} (downregulated with high A_n).

Pattern Learning

We can show the effect of this learning rule on pattern learning. We generate synaptic inputs from a grid of 200 input neurons for a single layer of 10 MSNs. On this grid we project two stripes of width 4 as a simple input pattern P_{learn} by adjusting the mean interspike interval (ISI) for the corresponding input neurons to a higher value ($ISI = 350$ ms for *on* vs. 750 ms for *off* neurons, see Fig. 5).

We apply the learning rule to each of the currents I_{Na} , I_{CaL} and I_{As} . This mimics changes in dopamine D1 receptor sensitivity, which targets these ion channels. Adaptation can be weaker or stronger, depending on learning time (e.g., $\sigma=0.01$, $t=20$ s (20 steps) (weak), $t=40$ s (40 steps) (strong)). After a number of steps, we achieve a distribution of μ -values that reflects the strength of the input (Table 3 A).

In Fig. 6, we obtain spike frequency histograms from the set of MS neurons under different conditions. Fig. 6 A shows the naive response to the input pattern P_{learn} - high activation in two medial areas. After adaptation, this response is increased (Fig. 6 B). When we apply a test input of a random noise pattern P_{noise} , we see that the learned pattern is still reflected in the spike histogram (Fig. 6 C). For positive learning, this process is theoretically unbounded, and only limited by the stepsize and the adaptation time. A saturation state could be defined to prevent unbounded learning, which would also allow to perform capacity calculations.

We should note that applying just one pattern continuously results in a very simple learning trajectory: each update results in a step change in the relevant ion channel currents. However, we also show that the effects of stepwise adaptation of individual ion channels do not necessarily lead to a completely parallel adaptation of firing rate. In Fig. 6 we see that adaptation is much stronger for high input rather than low

input neurons. In this case, θ at 11.5Hz is a fairly low value for neurons to continue to lower their firing rate with stepwise adaptation of the chosen ion channels. This shows the importance of using appropriate tuning ('harnessing') mechanisms to make highly nonlinear channels work in a purely linear learning context.

Clearly one of the results of learning is an altered spiking behavior of individual neurons dependent on their history. It is important to realize that this rule is based on neural activation, not synaptic input as a learning parameter - since synaptic input is constant during learning.

Positive and Negative Trace Learning

We show that this mechanism can be employed not only for positive trace learning, when excitability adaptation corresponds to frequency response, but also for negative trace learning, when excitability adaptation counteracts frequency response and approximates a target firing rate θ . This target rate could be set as a result of global inhibitory mechanisms corresponding to the expected mean A_i values under physiological stimulation. Accordingly, the neuron responds with decreases of excitability to high input ranges and increases of excitability to low input ranges (Fig. 8).

$$\begin{aligned}\Delta\mu &= h(A_n) = -\sigma & \text{if } A_n > \theta \\ \Delta\mu &= h(A_n) = \sigma & \text{if } A_n < \theta\end{aligned}\quad (6)$$

This emphasizes that "homeostatic" responses - adjusting excitability in the opposite direction to the level of input - can implement trace learning (pattern learning and feature extraction) as well.

Negative learning rule results in a mirror image of parameter values compared to positive learning, as shown in Table 3 B. The naive response is the same as before (Fig. 6 A). But here, after adaptation, the neurons have habituated to the input, and do not produce a strong response anymore (Fig. 7 A). When neurons are tested with P_{noise} , an inverse version of the original pattern appears (Fig. 7 B). Similarly, when we apply a different pattern P_{test} , we obtain a spike histogram, where the learned pattern is overlaid with the new input, resulting in a dampening of the frequency response for P_{test} (Fig. 7 C).

For both positive and negative traces, learning is pattern-specific, i.e. training with homogeneous, fluctuating (high-low) noise, such as P_{noise} , results in no adjustments (or computes an average). However, any prolonged sequence of neuron-selective stimulation results in neuron-selective patterns. This requires the population to be protected from prolonged stimulation with random patterns in a biological setting. We may assume most patterns to be meaningful and highly repetitive, while the neuron exists in a plastic state, while patterns may be random, when the neuron is not plastic (because it is stimulated with highly correlated or very low frequency input, saturated in its parameters or undergoes ion channel block by selected neuromodulators).

Discussion

Experimental results on induction of intrinsic plasticity

A number of experimental results show that intrinsic plasticity in MSNs may be prominently induced and regulated by intracellular calcium: It has been shown that e.g. the regulation of delayed rectifier K^+ -channels (Kv2.1 channels) is effectively performed by Ca^{2+} influx and calcineurin activation in cultured hippocampal neurons, which can be achieved by glutamate stimulation [Misonou et al., 2004]. The regulation concerns marked dephosphorylation (reduction of conductance) plus a shift in voltage-dependence. It has also been shown that 20 s of NMDA stimulation, or alternatively, increase of intracellular calcium, increases functional dopamine D1 receptor density at the membrane, which corresponds to an alteration in κ for D1 parameters, targeting a number of ion channels simultaneously [Scott et al., 2002]. For deep cerebellar neurons, there has recently been some direct evidence on the conditions that induce intrinsic plasticity. Here, alterations in intrinsic excitability can be induced by bursts of EPSPs and IPSPs, accompanied by dendritic calcium transients [Zhang et al., 2004]. In striatal MSNs, it has been determined that synaptic stimulation at 1 Hz does not cause significant calcium signals, but 10 Hz stimulation causes moderate

increases, and higher stimulation (up to 100Hz) significantly raises calcium levels [Bonsi et al., 2003].

In the simulations, neural activation (A_n) is estimated from the number of spikes generated, measured over the simulated behavior. In the model case, the membrane potential is not used as a separate parameter, because membrane potential and spiking behavior are closely linked. However, when a neuron exhibits prominent upstates (periods of high membrane voltages with a variable number of actual spikes), membrane potential may need to be treated as an additional, independent component of A_n , since a great part of the intracellular calcium signal in striatal MSNs is being generated from high-voltage activated NMDA and L-type calcium channels [Carter and Sabatini, 2004]. The number of spikes produced nonetheless seems important because of the phenomenon of backpropagating spikes. Backpropagating spikes enhance the calcium signal, thus providing a basis for a prominent role for spiking behavior, or firing rate, for defining intracellular calcium. The presence of backpropagation of spikes has recently been confirmed for MSNs [Carter and Sabatini, 2004].

In general, the induction of intrinsic plasticity may be linked not only to intracellular calcium. There exists an intricate intracellular system of interactions between diffusible substances like calcium and cAMP, as well as a number of crucial proteins (RGS, calcineurin, PKA, PKC, other kinases and phosphatases) for regulating receptor sensitivity and ion channel properties, which are furthermore influenced by NM receptor activation. Thus the learning parameter h may be analyzed as being dependent not only on A_n , but also on $[NM]$, and possibly even a third variable for a - slowly changing - intracellular state.

Synaptic vs. Intrinsic Plasticity

Learning by intrinsic excitability seems particularly suitable for striatal MSNs, since they have few lateral connections, which provide only a small part of their total input [Tepper et al., 2004]. When we have strong recurrent interaction, as in cortex, intrinsic excitability learning needs to adjust activation functions relative to each other, e.g. to ensure optimal distribution of activation functions. This probably happens in

the cortical maps, such as frequency maps in auditory cortex [Bao et al., 2001].

In hippocampus, synaptic and intrinsic modulation may potentiate each other (E-S potentiation, [Zhang and Linden, 2003]), but in other systems (e.g. striatum) antagonistic regulation may also exist (such as LTD combined with positive learning), with effects on the balance of synaptic vs. whole-cell localization for the storage of information.

Neuromodulation

When ion channels are regulated by neuromodulation, we can use a factor $[NM]\kappa$ - where $[NM]$ is the extracellular concentration of the ligand and κ the receptor sensitivity (see , Eq. 4). κ stands for the influence that a NM signal of a certain strength has on a particular ion channel, i.e. the degree of coupling between NM receptor ligand binding and ion channel modification [Scheler, 2004b]. Typically, a signal $[NM]$ will regulate several ion channels in parallel, but there may be different κ_i for each ion channel.

If activation function adaptation proceeds by NM-activated κ parameters, rather than unconditioned μ parameters, response to stimuli will consist of an early, non-modulated component, where the input pattern is reflected directly in the spiking frequency, and a later, modulated component, where habituation occurs for a learned pattern, or the stored pattern is reflected by overlaying a new stimulus and the stored pattern.

NM signals orchestrate both adjustments in activation function and synaptic input, with NM activation often depressing synapses, but increasing the variability in the activation function through selected conductance changes (activating κ -parameters). As a result, the input component of the signal is reduced in comparison to the stored intrinsic component after NM activation. Presumably, this has a dynamic component, such that for a short time after a strong signal there is an input-dominant phase which is then followed by an intrinsic-dominant phase.

Homeostasis, Permanence and Information Flow

There are different ideas at the present time what intrinsic plasticity can achieve within a network model of neuronal interaction. A recent review of intrinsic plasticity [Zhang and Linden, 2003] has left the authors wondering, whether IP acts mainly to maintain homeostasis, adapting to changes in synaptic strength by keeping neurons within certain ranges but without significant informational capacity, as in the model of [Stemmler and Koch, 1999]. However, as we have shown, homeostatic adaptation does not exclude information storage under conditions of conditional read-out. The synergy between synaptic and intrinsic plasticity may take different forms, beyond E-S potentiation. In contrast to [Stemmler and Koch, 1999, Zhang and Linden, 2003], [Destexhe and Marder, 2004] have listed many possible functions and roles of intrinsic adaptive plasticity, based on a review of experimental evidence in different systems.

We have greatly simplified the exposition here by concentrating on spike frequency as a major indicator of neural behavior. Certainly the type of firing (e.g. burst firing) is also under control of neuromodulators, and may be influenced by the distribution and density of ion channels. Single neuron computation is more complex than what can be shown with a single compartment model. In dendritic computation, the coupling of different compartments may be prominently affected by intrinsic plasticity. For instance, [Misonou et al., 2004] showed a loss of clustering for K⁺ channels on the membrane, induced by high glutamate stimulation, indicating a possible input-dependent regulation of dendritic integration.

A recent study on concurrent simulation of synaptic coupling parameters and intrinsic ion channel conductances has concluded that intrinsic and synaptic plasticity can achieve similar effects for network operation [Prinz and Marder, 2004]. We have suggested that synaptic and intrinsic plasticity can substitute for each other, and furthermore that this essential functional parallelism could be an indication for *information flow* over time from one modality to the other [Scheler, 2004a]. The direction of this informa-

tion flow may be from intrinsic to synaptic for the induction of permanent, morphological changes (such as dendritic spine morphology) - however the results of [Nelson et al., 2003] in cerebellum have also shown the possibility of permanent intrinsic plasticity (albeit in Purkinje cells which lack NMDA receptors and thus may be highly atypical neurons concerning learning properties). Clearly the interaction between synaptic and intrinsic plasticity is still an open question. Here we have shown a simple, local learning mechanism for intrinsic plasticity that allows to store pattern information without synaptic plasticity. This is different from theoretical approaches, where activation functions are only being modulated to optimize global measures of information transmission between neurons while the information is exclusively stored in synaptic weights. Further work will be needed to investigate the smooth integration of synaptic and intrinsic plasticity and their respective functions in different systems.

Conclusions

We wanted to show quantitatively that IP can have significant effects on spike frequency, dependent on the statistical structure of the input. In particular, low correlated input, or input during sensitive (high-voltage membrane) states induces the strongest variability of spike responses for different activation functions, while highly correlated input acts as drivers for neurons, eliminating subtle differences in activation function. We suggested that starting from a very general, natural format for a learning rule, which can be biologically motivated, we arrive at simple pattern learning, the basis for feature extraction, and realistic types of neural behavior: population-wide increases/decreases of neural firing rates to novel input stimuli, habituation to known stimuli and history-dependent distortions of individual stimuli. A significant application of this theoretical model exists in the observation of pervasive whole-cell adaptations in selected ion channels (I_{Na} , I_{CaL}) after cocaine sensitization [Hu et al., 2004, Zhang et al., 2002, Zhang et al., 1998], with implications of the type of learning that underlies addiction. This would reduce the dynamic range of intrinsic plasticity. Potentially, then, learning in striatum is mediated in part by in-

trinsic plasticity, and a reduction in inducible intrinsic plasticity or dynamic range of intrinsic plasticity after cocaine sensitization may contribute to the pathology of addiction.

References

- [Bao et al., 2001] Bao S, Chan VT, Merzenich MM (2001) Cortical remodelling induced by activity of ventral tegmental dopamine neurons. *Nature* 412, 79–83.
- [Bargas et al., 1994] Bargas J, Howe A, Eberwine J, Cao Y, Surmeier DJ (1994) Cellular and molecular characterization of Ca^{++} currents in acutely isolated, adult rat neostriatal neurons. *Journal of Neuroscience* 14 (11), 6667–6686.
- [Benucci et al., 2004] Benucci A, Verschure PF, König P (2004) Two-state membrane potential fluctuations driven by weak pairwise correlations. *Neural Computation* 16, 2351–78.
- [Bonsi et al., 2003] Bonsi P, Pisani A, Bernardi G, Calabresi P (2003) Stimulus frequency, calcium levels and striatal synaptic plasticity. *Neuroreport* 14, 419–22.
- [Carter and Sabatini, 2004] Carter AG, Sabatini BL (2004) State-dependent calcium signaling in dendritic spines of striatal medium spiny neurons. *Neuron* 44, 483–93.
- [Daoudal and Debanne, 2003] Daoudal G, Debanne D (2003) Long-Term Plasticity of Intrinsic Excitability: Learning Rules and Mechanisms. *Learning and Memory* 10, 456–465.
- [Destexhe and Marder, 2004] Destexhe A, Marder E (2004) Plasticity in single neuron and circuit computations. *Nature* 431, 789–95.
- [Gabel and Nisenbaum, 1998] Gabel LA, Nisenbaum ES (1998) Biophysical characterization and functional consequences of a slowly inactivating potassium current in neostriatal neurons. *Journal of Neurophysiology* 79, 1989–2002.
- [Goldman et al., 2001] Goldman MS, Golowasch J, Marder E, Abbott LF (2001) Global structure, robustness, and modulation of neuronal models. *Journal of Neuroscience* 21, 5229–38.
- [Gruber et al., 2003] Gruber AJ, Solla SA, Surmeier DJ, Houk JC (2003) Modulation of striatal single units by expected reward: a spiny neuron model displaying dopamine-induced bistability. *Journal of Neurophysiology* 90, 1095–114.
- [Hayashida and Ishida, 2004] Hayashida Y, Ishida AT (2004) Dopamine receptor activation can reduce voltage-gated Na^{+} current by modulating both entry into and recovery from inactivation. *Journal of Neurophysiology* 92, 3134–41.
- [Hu et al., 2004] Hu XT, Basu S, White FJ (2004) Repeated cocaine administration suppresses HVA- Ca^{2+} potentials and enhances activity of K^{+} channels in rat nucleus accumbens neurons. *Journal of Neurophysiology* 92, 1597–607.
- [LeMasson et al., 1993] LeMasson G, Marder E, Abbott LF, (1993) Activity-dependent regulation of conductances in model neurons. *Science* 259, 1915–7.
- [Mahon et al., 2003] Mahon S, Casassus G, Mulle C, Charpier S (2003) Spike-dependent intrinsic plasticity increases firing probability in rat striatal neurons in vivo. *Journal of Physiology* 550, 947–59.
- [Mahon et al., 2000a] Mahon S, Delord B, Deniau JM, Charpier S (2000) Intrinsic properties of rat striatal output neurones and time-dependent facilitation of cortical inputs in vivo. *Journal of Physiology* 527, 345–54.
- [Mahon et al., 2000b] Mahon S, Deniau JM, Charpier S, Delord B (2000) Role of a striatal slowly inactivating potassium current in short-term facilitation of corticostriatal inputs: a computer simulation study. *Journal of experimental Psychology – Learning Memory and Cognition* 7, 357–62.

- [Misonou et al., 2004] Misonou H, Mohapatra DP, Park EW, Leung V, Zhen D, Misonou K, Anderson AE, Trimmer JS (2004) Regulation of ion channel localization and phosphorylation by neuronal activity. *Nature Neuroscience* 7, 711–8.
- [Moyer et al., 1996] Moyer JRJ, Thompson LT, Disterhoft, JF (1996) Trace eyeblink conditioning increases CA1 excitability in a transient and learning-specific manner. *Journal of Neuroscience* 16, 5536–46.
- [Nelson et al., 2003] Nelson AB, Krispel CM, Sekirnjak C, du Lac S (2003) Long-lasting increases in intrinsic excitability triggered by inhibition. *Neuron* 40, 609–20.
- [Nisenbaum et al., 1998] Nisenbaum ES, Mermelstein PG, Wilson CJ, Surmeier DJ (1998) Selective blockade of a slowly inactivating potassium current in striatal neurons by (+/-) 6-chloro-APB hydrobromide (SKF82958). *Synapse* 29, 213–24.
- [Nisenbaum and Wilson, 1995] Nisenbaum ES, Wilson CJ (1995) Potassium currents responsible for inward and outward rectification in rat neostriatal spiny projection neurons. *Journal of Neuroscience* 15, 4449–63.
- [Onn et al., 2003] Onn SP, Fienberg AA, Grace AA (2003) Dopamine modulation of membrane excitability in striatal spiny neurons is altered in DARPP-32 knockout mice. *Journal of Pharmacology and Experimental Therapeutics* 306, 870–9.
- [Onn et al., 2000] Onn SP, West AR, Grace AA (2000) Dopamine-mediated regulation of striatal neuronal and network interactions. *Trends in Neuroscience* 23, S48–56.
- [Prinz and Marder, 2004] Prinz A, Marder E (2004) Similar network activity from disparate circuit parameters. *Nature Neuroscience* 431, 789–95.
- [Sachdev et al., 2004] Sachdev RNS, Ebner FF, Wilson CJ (2004) Effect of subthreshold up and down states on the whisker-evoked response in somatosensory cortex. *Journal of Neurophysiology* 92, 3511–21.
- [Scheler, 2004a] Scheler G (2004) Complex feature construction by neuronal abstraction. Society of Neuroscience Meeting.
- [Scheler, 2004b] Scheler G (2004) Regulation of neuromodulator receptor efficacy—implications for whole-neuron and synaptic plasticity. *Progress in Neurobiology* 72, 399–415.
- [Schreurs et al., 1998] Schreurs BG, Gusev PA, Tomasic D, Alkon DL, Shi T (1998) Intracellular correlates of acquisition and long-term memory of classical conditioning in Purkinje cell dendrites in slices of rabbit cerebellar lobule HVI. *Journal of Neuroscience* 18, 5498–507.
- [Scott et al., 2002] Scott L, Kruse MS, Forssberg H, Brismar H, Greengard P, Aperia A (2002) Selective up-regulation of dopamine D1 receptors in dendritic spines by NMDA receptor activation. *Proceedings of the National Academy of the Sciences U S A* 99, 1661–4.
- [Stemmler and Koch, 1999] Stemmler M, Koch C (1999) How voltage-dependent conductances can adapt to maximize the information encoded by neuronal firing rate. *Nature Neuroscience* 2, 521–7.
- [Surmeier et al., 1989] Surmeier DJ, Bargas J, Kitai ST (1989) Two types of A-current differing in voltage-dependence are expressed by neurons of the rat neostriatum. *Neuroscience Letters* 103, 331–7.
- [Tepper et al., 2004] Tepper JM, Koos T, Wilson CJ (2004) GABAergic microcircuits in the neostriatum. *Trends in Neuroscience* 27, 662–9.
- [Thomas et al., 2001] Thomas MJ, Beurrier C, Bonci A, Malenka RC (2001) Long-term depression in the nucleus accumbens: a neural correlate of behavioral sensitization to cocaine. *Nature Neuroscience* 4, 1217–23.

- [Thompson et al., 1996] Thompson LT, Moyer JRJ, Disterhoft JF (1996) Transient changes in excitability of rabbit CA3 neurons with a time course appropriate to support memory consolidation. *Journal of Neurophysiology* 76, 1836–49.
- [Tsubo et al., 2004] Tsubo Y, Kaneko T, Shinomoto S (2004) Predicting spike timings of current-injected neurons. *Neural Networks* 17, 165–73.
- [Wang and Buzsaki, 1996] Wang XJ, Buzsaki G (1996) Gamma oscillation by synaptic inhibition in a hippocampal interneuronal network model. *Journal of Neuroscience* 16, 6402–13.
- [Wickens and Wilson, 1998] Wickens JR, Wilson CJ (1998) Regulation of action-potential firing in spiny neurons of the rat neostriatum in vivo. *Journal of Neurophysiology* 79, 2358–64.
- [Wilson and Kawaguchi, 1996] Wilson CJ, Kawaguchi Y (1996) The origins of two-state spontaneous membrane potential fluctuations of neostriatal spiny neurons. *Journal of Neuroscience* 16, 2397–410.
- [Zhang and Linden, 2003] Zhang W, Linden DJ (2003) The other side of the engram: experience-driven changes in neuronal intrinsic excitability. *Nature Reviews Neuroscience* 4, 885–900.
- [Zhang et al., 2004] Zhang W, Shin JH, Linden DJ (2004) Persistent changes in the intrinsic excitability of rat deep cerebellar nuclear neurones induced by EPSP or IPSP bursts. *Journal of Physiology* 561, 703–19.
- [Zhang et al., 2002] Zhang XF, Cooper DC, White FJ (2002) Repeated cocaine treatment decreases whole-cell calcium current in rat nucleus accumbens neurons. *Journal of Pharmacology and Experimental Therapeutics* 301, 1119–25.
- [Zhang et al., 1998] Zhang XF, Hu XT, White FJ (1998) Whole-cell plasticity in cocaine withdrawal: reduced sodium currents in nucleus accumbens neurons. *Journal Neuroscience* 18, 488–98.

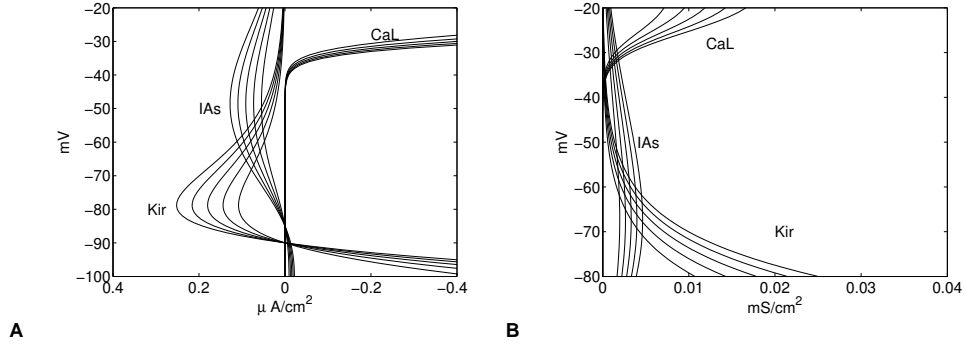


Figure 1: Variable factors ($\mu = \{0.6 \dots 1.4\}$) for the slowly inactivating K^+ -channel ($Kv1.2$, I_{As}), the L-type calcium channel (I_{CaL}), and the inward rectifying K+ channel (I_{Kir}) are shown at different membrane voltages V_m (A) in an I-V plot, (B) as variability in conductance.

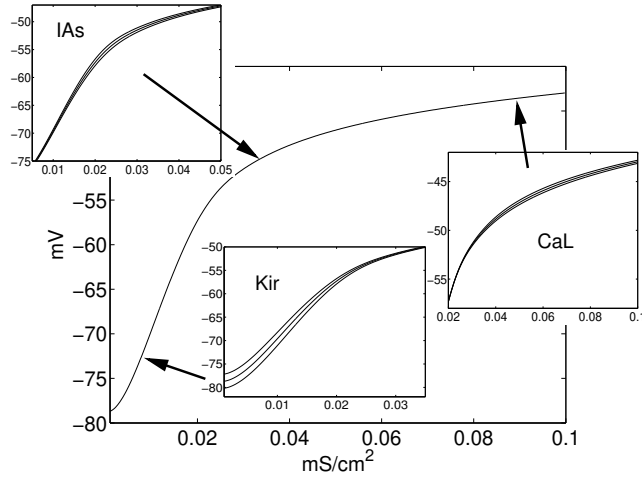


Figure 2: Variable factors ($\mu = \{0.6 \dots 1.4\}$) for I_{As} , I_{CaL} , and I_{Kir} as components of the activation function (g_s vs. V_m). The activation function is defined as the membrane voltage response for different injected (synaptic) conductances (g_s), and computed by solving Eq3 for the membrane voltage V_m .

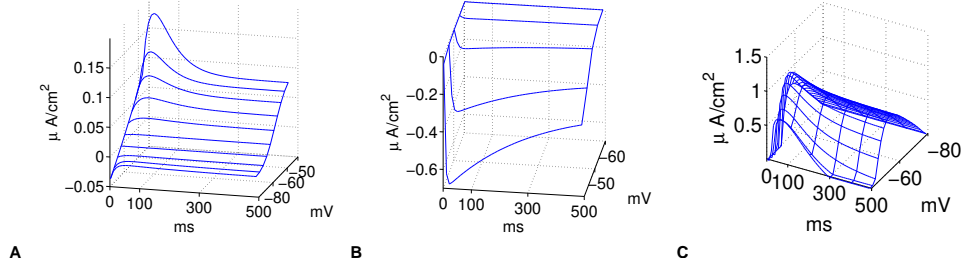


Figure 3: Activation-inactivation (temporal) dynamics (A) for the slow A channel I_{As} (B) the L-type Ca channel I_{CaL} , and (C) for the set of ion channels used in the standard MSN model. We see a rise time due to I_{As} and overlapping inactivation dynamics in the -55 to -40 mV range.

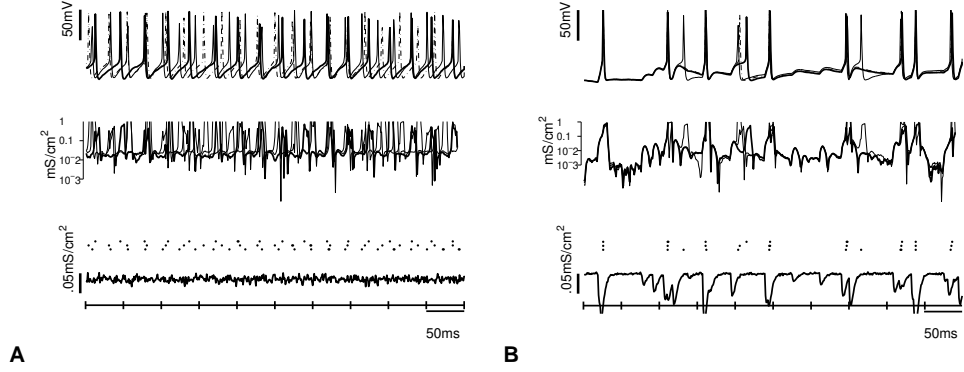


Figure 4: Response to inputs generated from $N = 80$ neurons with independent Poisson processes using different correlations parameters $W = 0.2, 0.9$ (A,B). Three slightly different neurons with $\mu_{As} = 1.1, 1.3, 1.5$ are shown under BOTH conditions. (A) Response variability and different firing rates for each neuron (here: 20,26,40 Hz) occur with distributed (low correlation) input. (B) Highly correlated input produces reliable spiking and by implication a single firing rate (20Hz). The upper panel shows the membrane voltage, the middle panel shows the membrane conductances, and the lower panel shows the synaptic input as conductance.

I	p	q	\bar{g}	λ_α	V_c^α	V_i^α	$Eq(\alpha)$	λ_β	V_c^β	V_i^β	$Eq(\beta)$	E^{rev}
Na (m)	3		35	0.1	10	-28	3	4.0	18	-53	1	55
Na (h)		1		0.07	20	-51	1	1	10	-21	2	
K	4		6	0.01	10	-34	3	0.125	80	-44	1	-90
CaL (m)	2		0.01	0.06	3.8	-40	3	0.94	17	-88	1	140
CaL (h)		1		4.6e-4	50	-26	1	6.5e-3	28	-28	2	
leak			0.04									-75

Table 1: Parameter values for I_{Na} , I_K , I_{leak} as in (Wang and Buzsaki, 1996) I_{CaL} as in (Bargas et al., 1994; Tsubo et al., 2004)

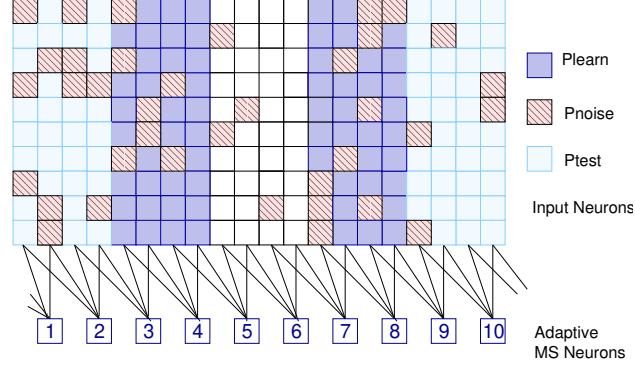


Figure 5: Pattern learning: 200 input neurons (arranged as 20X10), 10 learning neurons, and definitions for 3 patterns. Only 37 of 80 data points for P_{noise} are shown.

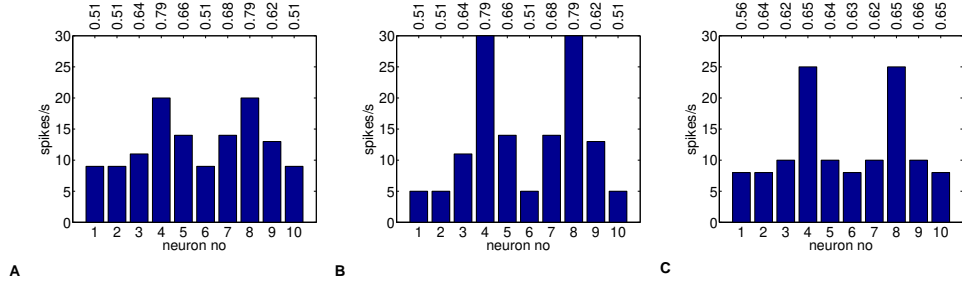


Figure 6: Positive pattern learning: spike frequency histograms for 10 adaptive neurons ($\theta=11.5\text{Hz}$) (A) response of naive neurons to P_{learn} (B) response of P_{learn} -adapted neurons to P_{learn} (C) P_{learn} -adapted neurons tested with P_{noise} . Average synaptic input (nA/cm^2) for each neuron is shown on top. Responses in (A) and (B) to the same input P_{learn} are different, a pattern similar to P_{learn} emerges in response to uniform (noise) pattern input in (C).

I	p	q	\bar{g}	V_c^{m0}	V_i^{m0}	$Eq(m0)$	V_c^{h0}	V_i^{h0}	$Eq(h0)$	τ_m	τ_h	E^{rev}
Kir	1		0.15	-10	-100	2				<0.01	<0.01	-90
Af	1	1	0.09	7.5	-33	2	-7.6	-70	2	1	25	-73
As	1	1	0.32	13.3	-25.6	2	-10.4	-78.8	2	(a)	(b)	-85
Nas	1		0.11	9.4	-16.0	2				(c)	<0.01	40

Table 2: Parameter values for potassium channels I_{Kir} , I_{Af} , I_{As} and a slow sodium channel I_{Nas} cf. (Mahon et al., 2000b; Gruber et al., 2003), where (a) $\tau_m = 131.4/(\exp(-(V_m + 37.4)/27.3) + \exp((V_m + 37.4)/27.3))$ (b) $\tau_h = 179.0 + 293.0 * \exp(-((V_m + 38.2)/28)^2) * ((V_m + 38.2)/28)$ (c) $\tau_m = 637.8/(\exp(-(V_m + 33.5)/26.3) + \exp((V_m + 33.5)/26.3))$

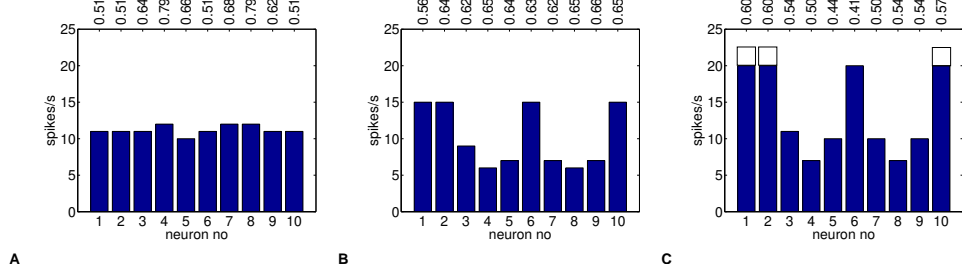


Figure 7: Negative pattern learning: spike frequency histograms for 10 adaptive neurons ($\theta=11.5\text{Hz}$) (A) habituation for neurons adapted to P_{learn} , (B) an inverse pattern for P_{learn} -adapted neurons tested with P_{noise} and (C) interference (dampening of response) for a new pattern P_{test} (naive: line-drawn bars, adaptive: filled bars). Average synaptic input (nA/cm^2) for each neuron is shown on top. (A) shows a uniform response to patterned synaptic input and (B) a patterned response to uniform (noise) input. (C) shows a difference of response for naive vs. P_{learn} -adapted neurons to a new pattern P_{test} .

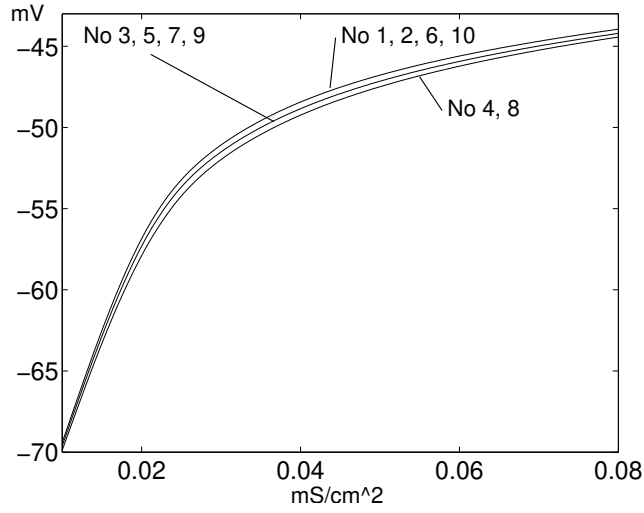


Figure 8: Negative pattern learning: Learning results in different activation functions for high (4,8), medium (3,5,7,9) and low (1,2,6,10) input.

no	μ_{CaL}	μ_{As}	μ_{Na}
1	0.9/0.8	1.2/1.4	0.9/0.8
2	0.9/0.8	1.2/1.4	0.9/0.8
3	1.0	1.0	1.0
4	1.1/1.2	0.8/0.6	1.1/1.2
5	1.0	1.0	1.0
6	0.9/0.8	1.2/1.4	0.9/0.8
7	1.0	1.0	1.0
8	0.9/0.8	1.2/1.4	0.9/0.8
9	1.0	1.0	1.0
10	0.9/0.8	1.2/1.4	0.9/0.8

A

no	μ_{CaL}	μ_{As}	μ_{Na}
1	1.4	0.7	1.0
2	1.4	0.7	1.1
3	0.9	1.1	1.0
4	0.6	1.4	0.8
5	1.1	0.8	0.9
6	1.4	0.7	1.1
7	1.1	0.8	0.9
8	0.7	1.4	0.8
9	1.0	0.9	0.9
10	1.4	0.7	1.1

B

Table 3: Pattern learning: Parameter values (A) for positive learning with (weak/strong) adaptation of μ values and (B) negative learning. CaL and Na channels are adapted in the opposite direction to K channels.